Revista Ciência Agronômica, v. 56, e202292588, 2025
Centro de Ciências Agrárias - Universidade Federal do Ceará, Fortaleza, CE
www.ccarevista.ufc.br

Scientific Article
ISSN 1806-6690

Effect of indices on desertification risk: spatial and hierarchical approach using multinomial logistic regression[1]

Thiago Costa dos Santos[2]*, Adunias dos Santos Teixeira[3], Luis Clenio Jário Moreira[4], Raul Shiso Toma[2]

ABSTRACT - Desertification is the degradation process caused by climatic conditions and human activities that results in loss of soil productivity and decline in vegetation growth in the long term. Several indices related to vegetation, soil and climate are used to monitor desertification, but few studies explore qualitative and quantitative aspects of indices on desertification on spatial and hierarchical scale. This study aims to identify and measure indices related to increased risk of desertification on global, local and hierarchical scales using multinomial logistic regression models. Images from TM, ETM+ and OLI sensor from 1997 to 2018 in the end of dry and rainy seasons were used to quantify NDVI, TGSI, albedo, temperature, aridity index, evapotranspiration and precipitation on global spatial scale (Irauçuba Centro Norte) and local spatial scale (Miraíma, Canindé, Irauçuba and Santa Quitéria). GISD was calculated by geometric mean of weighted indices and segmented into 8 classes of susceptibility to desertification (hierarchical scale). The results showed that the best models were obtained on local scale and for the end of the rainy season. Temperature proved to be the most important variable for increased risk of desertification on global, local and hierarchical scales. Therefore, the increase in the risk of desertification in the studied areas is due to human activities of deforestation, overgrazing and fire. These factors contributed to reduction of vegetation cover and increase in temperature, changing the microclimatic, which led to decline in precipitation and worsening of desertification.

Key words: Precipitation. Temperature. Deforestation. Microclimate.

DOI: 10.5935/1806-6690.20250009
Editor-in-Chief: Prof. Adriel Fonseca - adrielff@gmail.com
*Author for correspondence
Received for publication 19/12/2022; approved on 21/09/23
[1]Work extracted from the thesis of the first author presented to the Graduate Program in Soil Science, Federal University of Ceará/UFC
[2]Department of Soil Sciences, Federal University of Ceará (UFC), Fortaleza-CE, Brazil, thiagoengagronomo@hotmail.com (ORCID ID 0000 0001 6749 850X), raulstoma@ufc.br (ORCID ID 0000 0001 5585 6832)
[3]Department of Agricultural Engineering, Universidade Federal do Ceara (UFC), Fortaleza-CE, Brazil, adunias@ufc.br (ORCID ID 0000 0002 1480 0944)
[4]Federal Institute of Education, Science and Technology of Ceará (IFCE), Limoeiro do Norte-CE, Brazil, cleniojario@gmail.com (ORCID ID 0000 0001 9918 9744)

INTRODUCTION

Desertification is the process of degradation that occurs in regions of arid, semi-arid and dry sub-humid climate as a result of anthropogenic pressure caused by land use and occupation activities that dispense with the sustainable and conservational use of natural resources, leading in the long term to deterioration of soil and vegetation quality, resulting in changes in temperature and energy flow between the soil and atmosphere, culminating in reductions in precipitation and moisture available to plants and increasing water scarcity and desertification (Ning *et al*., 2021; Zolotokrylin; Brito-Castillo; Titkova, 2020).

In Brazil, desertified areas are concentrated in the northeast region, characterized by a semi-arid climate that occupies 13% of the Brazilian territory, and a population density of more than 20 people per km^2, which increases the pressure on the natural resources of these areas by the action of deforestation, fires, overgrazing and subsistence agriculture, resulting in the removal of native vegetation and favoring erosion and degradation processes, leading to climate change and ultimately to desertification (Perez-Marin *et al*., 2022; Souza *et al*., 2020).

Remote sensing images have been widely used for desertification studies, as the temporal and spectral resolution of the sensor allows periodic observations of changes in the Earth's surface through the evaluation and quantification of multiple bands and spectral indices whose responses are altered as a result of desertification (Santos *et al*., 2021).

Normalized Difference Vegetation Index (NDVI), Topsoil Grain Size Index (TGSI), albedo, precipitation, temperature, evapotranspiration and aridity index are remote indices frequently used in desertification studies, as they represent changes in vegetation growth conditions, energy balance between soil and atmosphere and precipitation as a result of deforestation activities, as well as fires and overgrazing, which reduce vegetation cover and precipitation, increasing albedo and temperature, and intensifying desertification (Djeddaoui; Chadli; Gloaguen, 2017; Ferreira *et al*., 2018; Ning *et al*., 2021; Zolotokrylin; Brito-Castillo; Titkova, 2020).

Spectral indices obtained by remote sensing are used in deterministic models of susceptibility to desertification, for instance, MEDALUS (Mediterranean Desertification and Land Use), proposed by Kosmas, Kirkby and Geeson (1999), which is based on the physical characterization of vegetation, soil, climate and socioeconomic aspects, based on weightings of indices calibrated in loco, which compromises its applicability at a global level, resulting in less accurate models that do not show the contribution of each index to the risk of desertification (Li, P *et al*., 2022).

Several models have been used to identify and quantify the indices that increase or reduce the risk of desertification, considering the spatial scale of the mapped areas and the hierarchy of the risk of desertification (Djeddaoui; Chadli; Gloaguen, 2017; Li, G *et al*., 2022; Mihi; Ghazela; Wissal, 2022). However, Brazil still lacks models that explore the effects of different indices on desertification risks, considering the spatial scale of the mapped areas and the hierarchy of susceptibility to desertification. Therefore, this article aims to identify and quantify the indices related to the increased risk of desertification at global, local and hierarchical scales using multinomial logistic regression models.

MATERIAL AND METHODS

Study Area

The approach to susceptibility to desertification at spatial and hierarchical scales aims to quantify the contribution of indices related to vegetation, climate and soil at global and local spatial scales at different levels of susceptibility to desertification, using multinomial logistic regression (MLR) models.

The global scale refers to the region of Irauçuba Centro Norte (ICN) with coordinates 3°35' and 4°44' S and 39° 38' and 39°63' W and an area of 9,579.21 km^2; the local scale refers to each municipality that is part of the region of Irauçuba Centro Norte: Miraíma (latitude of 3°34' S and longitude 39°58' W, with an area of 699.59 km^2); Canindé (latitude of 4°21' S and longitude of 39°18' W, with an area of 3,218.42 km^2); Irauçuba (latitude of 3°44' S and longitude of 39°47' W, with an area of 1,461.22 km^2) and Santa Quitéria (latitude of 4°19' S and longitude of 40°09' W, with an area of 4,260.50 km^2) (Figure 1).

The region of Irauçuba Centro Norte has vegetation of the shrubby Caatinga type with herbaceous cover, with forage potential, favoring extensive livestock farming, which occupies 67% of the area, contributing to degradation and intensification of erosion (Sousa *et al*., 2012). According to Köppen's classification, the region has a Bsh'w climate, hot semi-arid, high variability of precipitation, average annual temperature of 26.3 °C and precipitation below 500 mm.

Regarding geomorphological aspects, Irauçuba Centro Norte is delimited by the Sertões and Serras. Sertões comprise Sobral, Canindé, Santa Quitéria, Miraíma and Irauçuba and are characterized by having from pediplains to moderately dissected surfaces with rainfall between 560 and 850 mm, and soils classified as *Neossolos Litólicos* [Entisols] (on low slopes and residual ridges), *LUVISSOLOS* [Alfisols] (shallow hills), *PLANOSSOLOS* [Alfisols] and *Neossolos*

Flúvicos [Entisols] (on valley bottoms). The mountain areas are: Matas, Rosário, Machado, Uruburetama and Baturité, with rainfall between 550 and 900 mm and soils classified as *ARGISSOLOS VERMELHOS AMARELOS* [Ultisols], *Neossolos Litólicos* [Entisols] and *Neossolos Flúvicos* [Entisols] (FUNCEME, 2015).

Methodology and procedures

The sequence of methodological procedures adopted in this article is presented in the flowchart in Figure 2.

1. Acquisition, processing and calculation of indices on global and local scales

Images from the Landsat 05 (TM), Landsat 07 (ETM+) and Landsat 08 (OLI and TIRS) satellites referring to orbits/points 217/63, 218/62 and 218/63 were obtained from the United States Geological Survey (USGS) platform. Cloud cover and precipitation observed in dry and rainy seasons were used as criteria for image selection. The years of the time series between 1997 and 2018 were subdivided into: ER (End Rainy) corresponding to the final period of the rainy season (October) and ED (End Dry) referring to the final period of the dry season (July).

Figure 1 - State of Ceará (1). Global (2) and local (3) spatial location

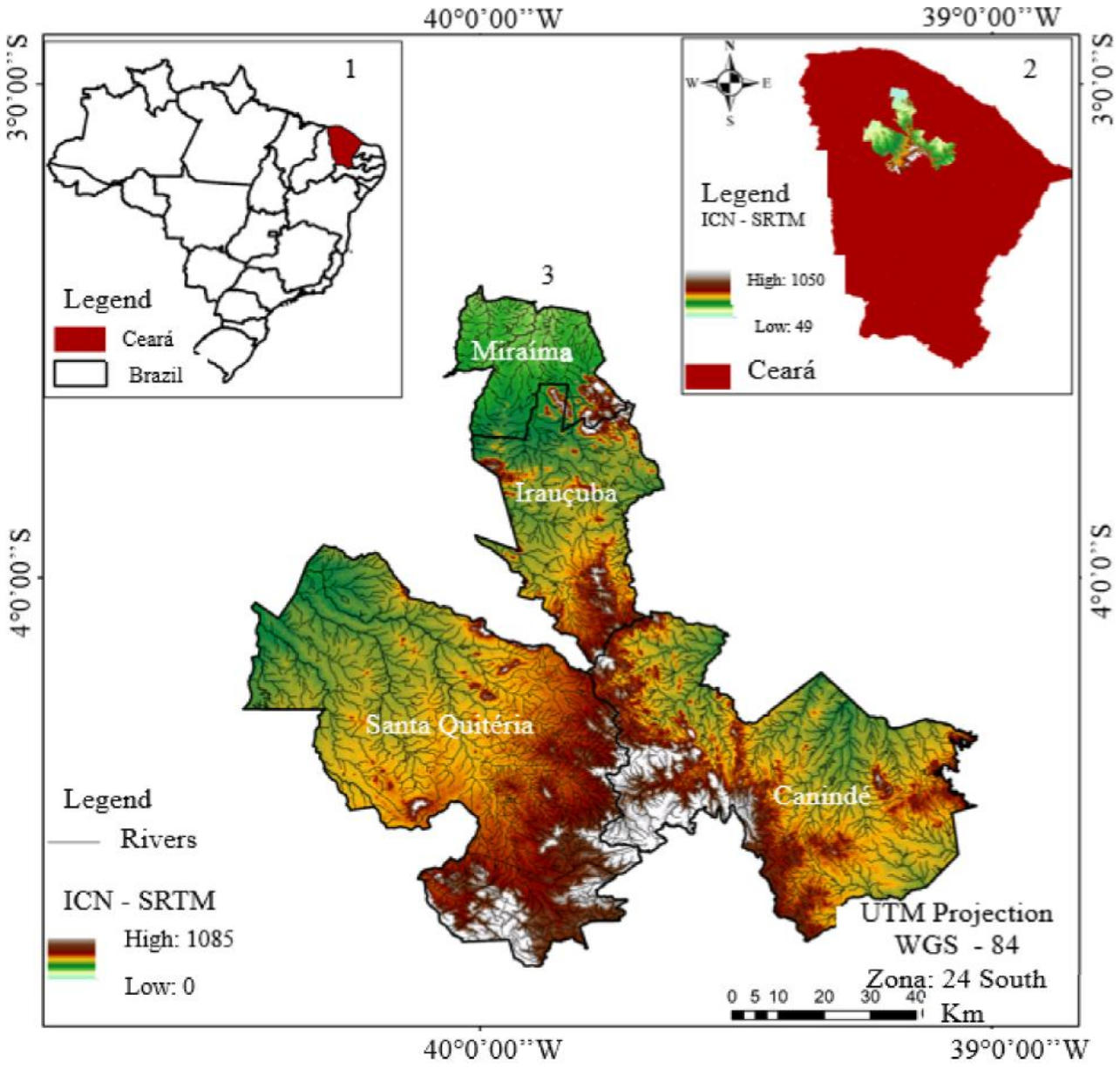

The images were reprojected to Zone 24 SOUTH and DATUM WGS – 84, then subjected to atmospheric and geometric correction, mosaicking (joining of images) and clipping (cutting of the study areas); all these procedures were done in Envi® 4.8. The indices were calculated on a global scale (Irauçuba Centro Norte) and on a local scale (Miraíma, Irauçuba, Santa Quitéria and Canindé) using the formulas presented in Table 1.

Figure 2 - Methodological steps of the study

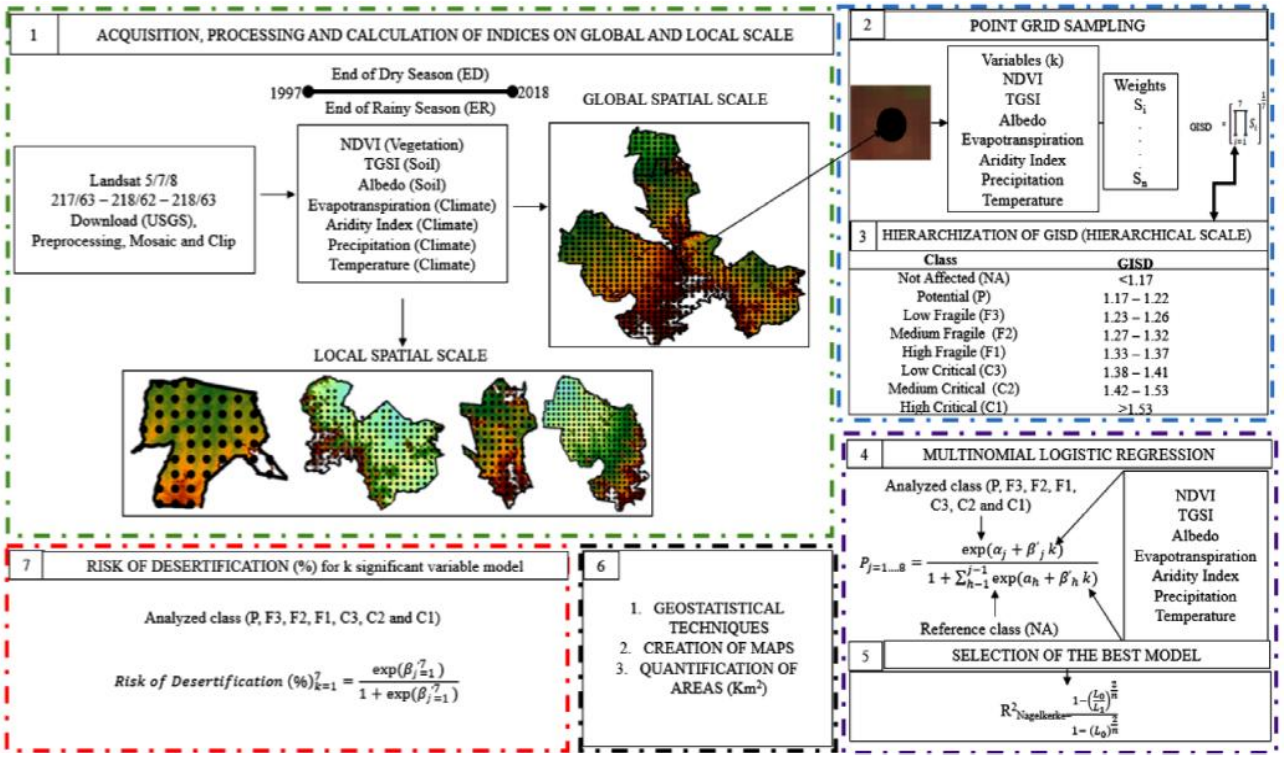

Table 1 - Formulas of the indices used in this experiment

Index	Formula	Order
NDVI	$\frac{p\lambda_4 + p\lambda_3}{p\lambda_4 - p\lambda_3}$	1
TGSI	$\frac{(p\lambda_3 - p\lambda_1)}{p\lambda_3 + p\lambda_2 + p\lambda_1}$	2
Albedo	$\sum_{n=1}^{6}(p\lambda_i . \omega\lambda_i)$	3
Precipitation	$\sum_{n=1}^{6}(Z_i / h^{\beta} ij) / \sum_{i=1}^{n}(1 / h^{\beta} ij)$	4
Aridity Index	$\frac{Pr}{ETP}$	5
Evapotranspiration	$\frac{3600.LE}{(\lambda)}$	6
Surface Temperature	$\frac{(K_2)}{\ln(\varepsilon_0 . K_1) + 1}$	7

$p\lambda_{1,2,3}$ and $_4$: reflectances of the blue, green, red, and near-infrared bands, respectively; ω: coefficients of the bands used to calculate the albedo; Z_i: known precipitation value of point i; h_{ij} distance from point i to j; β: parameter of power equal to 2; P_r: interpolated precipitation (mm); ETP: monthly potential evapotranspiration (mm); LE: latent heat flux (W.m^{-2}); λ: Latent heat of vaporization of water (2.45x106 J.kg^{-1}); K_1 and K_2: calibration parameters: K_1 = 607.76 W m^{-2} sr^{-1}μm^{-1} and K_2 = 1260.56 W m^{-2} sr^{-1}μm^{-1}; ε_0: emissivity relative to the pixel (dimensionless)

2. Point-grid sampling

Global and local GISD were constructed by delimiting a grid of equidistant points, which served for sampling the calculated indices. For the construction of global GISD, 649 sampling points were selected from Irauçuba Centro Norte; for the local GISD of Miraíma, Canindé, Irauçuba and Santa Quitéria, 50, 215, 96 and 288 sample points were selected, respectively. Thus, each sampled point carries the information of the 7 calculated indices that were weighted according to Xu, You and Xia (2019) and Sharma, Raj and Somawat (2021), as presented in Table 2.

With the weight associated with each index, the geometric desertification susceptibility index (GISD) adapted from the MEDALUS methodology proposed by Karamesouti, Panagos and Kosmas (2018) was calculated using Equation 8:

$$GISD = \left(II_{7}{}_{n=1} Si\right) 1/7 \quad (8)$$

Where:

n: number of variables used to determine susceptibility to desertification, which in this study ranged from 1 to 7;

S_i: weight assigned to the value of the index according to the level of susceptibility to desertification;

∏: product of the weights of each index.

3. Hierarchization of GISD (Hierarchical Scale)

Hierarchization of GISD was based on the study conducted by Uzuner and Dengiz (2020), as presented in Table 3.

4. Application of the multinomial logistic regression model

The multinomial logistic regression model was applied according to Equation 9:

$$P_{j=1\ldots8} = \frac{\exp\left(\alpha_j + \beta_j' k\right)}{1 + \sum_{h-1}^{j-1} \exp\left(\alpha_h + \beta_h' k\right)} \quad (9)$$

Where:

P_j: probability value associated with j-th class;

exp (α_j+β_j, K): exponential of the logistic model associated with the studied class (P, F3, F2, F1, C3, C2, and C1);

exp (α_j+β_h, K): exponential of the logistic model associated with the reference class (NA);

K: explanatory variables of the model.

5. Selection of the best model

The best model was defined by quantifying the Nagelkerke pseudo R^2 (the closer to 1, the better its performance), calculated using Equation 10:

$$R^2_{Nagel\,ker\,ke} = \frac{1 - \left(\frac{L_0}{L_1}\right)^{\frac{2}{n}}}{1 - (L_0)^{\frac{2}{n}}} \quad (10)$$

Where:

L_0: logistic model with only intercept;

L_1: logistic model with significant variables.

Table 2 - Weighting of indices

Criterion	Index	Intervals	Weight	Units
Vegetation	NDVI	<=0.3	2	Dimensionless
		0.3<NDVI<=0.4	1.5	
		NDVI>0.4	1.0	
Soil	TGSI	-0.01<=TGSI<=0	1.0	Dimensionless
		TGSI>0	2.0	
	albedo	<=0.1	1	Dimensionless
		0.1<albedo<=0.20	1.5	
		albedo>0.20	2	
Climate	aridity index	aridity index <0.1	2	Dimensionless
		0.10<= aridity index <1.0	1.5	
	precipitation	precipitation <=150	2	mm
		150< precipitation <=300	1.5	
		precipitation >300	1	
	evapotranspiration	evapotranspiration <0.41	1	mm/h
		0.41<= evapotranspiration <=0.55	1.5	
		0.55< evapotranspiration <1	2	
	temperature	temperature<25.3 °C	1	Celsius
		25.3 °C <=temperature<=41.5 °C	2	

Table 3 - Hierarchization of GISD

Class	GISD
Not Affected (NA)	1.17
Potential (P)	1.17 - 1.22
Low Fragile (F3)	1.23 - 1.26
Medium Fragile (F2)	1.27 - 1.32
High Fragile (F1)	1.33 - 1.37
Low Critical (C3)	1.38 - 1.41
Medium Critical (C2)	1.42 - 1.53
High Critical (C1)	>1.53

6. Geostatistical techniques, creation of maps and quantification of areas

Geostatistical techniques were used to spatialize GISD, making it possible to obtain representative maps of the different classes of susceptibility to desertification, and then the areas in km² were calculated. All of these steps were done in ArcGis version 10.5.

7. Risk of desertification (%)

The risk of desertification in percentage values (RD) for k significant variable was measured using Equation 11:

$$RD(\%)_{k=1}^{7} = \frac{\exp\left(\beta_{j=1}^{7}\right)}{1+\exp\left(\beta_{j=1}^{7}\right)} \quad (11)$$

Where:

K: explanatory variables;

exp ($\beta^{7}_{j,}$=1): exponential of the coefficient β referring to the explanatory variable k that was significant in the model.

RESULTS AND DISCUSSION

The MLR models that showed the highest $R^2_{nagelkerke}$ on global, local and hierarchical scales, as well as the vegetation, climate and soil indices that were significant for the prediction of desertification risk, are presented in Table 4.

The MLR showed lower $R^2_{Nagelkerke}$ in Irauçuba Centro Norte (global scale); the model obtained at the end of the dry season was able to explain 78.80% of the variability in the risk of desertification. The MLR models obtained at the end of the rainy season and referring to Miraíma, Canindé, Irauçuba and Santa Quitéria (local scale) showed higher $R^2_{Nagelkerke}$, explaining between 85.50% and 90.40% of the variability in the risk of desertification.

The desertification susceptibility classes in Miraíma, Canindé, Irauçuba, Santa Quitéria and Irauçuba Centro Norte are presented in Figure 3.

The GISD map obtained in 2005ER for Miraíma showed that class C2 occupied 57.49% of its territory, followed by C1 with 30.46%, C3 with 8.72% and F1 occupying just over 3% of the area. The MLR model showed that the temperature was significant (p-value < 0.05) for classes F1 (High Fragile) and C1 (High Critical), showing a positive coefficient, which indicates that the increase in temperature increased the risk of desertification by 54.25% for F1 and by 90.35% for C1.

In the F1 class, the indices had the following ranges: NDVI (0.1304 - 0.4099); TGSI (0.0367 - 0.3566); albedo (0.0570 - 0.1626); aridity index (0.1638 - 0.5346); precipitation (194.06 mm - 633.46 mm); evapotranspiration (0 - 0.5409 mm/h) and temperature (18.89 °C - 33.83 °C). For class C1, the indices had the following ranges: NDVI (0.1207 - 0.3722); TGSI (0.0672 - 0.2821); albedo (0.0527 - 0.2195); aridity index (0.1473 - 0.5115); precipitation (174.60 mm - 606.10 mm); evapotranspiration (0.1204 mm/h - 0.9096 mm/h) and temperature (27.44 °C - 36.72 °C).

In Canindé, the GISD map of 1998ER showed that classes F3, F2, F1 and C3 occupied less than 5%, while classes C2 and C1 occupied 23.37% and 63.20%, respectively. Temperature was significant (p-value < 0.05) and showed positive coefficients for classes F2, F1, C2 and C1, indicating that the increase of 1 degree Celsius in temperature increased the risks of desertification by 57.10%, 70.05%, 78.55% and 89.45%, respectively.

In the F2 class, the indices showed the following ranges: NDVI (0.4032 - 0.6095); TGSI (0.1491 – 0.2692); albedo (0.0538 - 0.1060); temperature (22.56 °C – 30.89 °C); aridity index (0.0610 – 0.1444); precipitation (151.00 mm – 357.47 mm) and evapotranspiration (0 – 0.3828 mm/h); while in F1 the indices ranged as follows: NDVI (0.3067 – 0.5673);

TGSI (0.1616 – 0.3203); albedo (0.0497 – 0.0996); temperature (23.46 °C – 31.31 °C); aridity index (0.0129 – 0.1704); precipitation (31.81 mm – 421.73 mm) and evapotranspiration (0 – 0.3629 mm/h). For class C2, the ranges were: NDVI (0.2137 – 0.5959); TGSI (0.1249 – 0.3726); albedo (0.0474 – 0.1659); temperature (22.11 °C – 31.74 °C); aridity index (0 – 0.1936); precipitation (0 – 479.08 mm) and evapotranspiration (0 – 0.3880 mm/h); in relation to class C1, the indices ranged as follows: NDVI (0.1748 – 0.4587); TGSI (0.0711 – 0.3312); albedo (0.0649 – 0.2144); temperature (25.69 °C – 32.16 °C); aridity index (0 – 0.1211); precipitation (0 – 299.72 mm) and evapotranspiration (0 – 0.3969 mm/h).

Table 4 - Variables and their effects on desertification risk on a global, local and hierarchical scale

Area/Period	$R^2_{Nagelkerke}$	Classes	Variables	(β)	Probability of Risk (%)
Miraíma (2005ER)	0.897	F1	Temperature	0.171	54.25
		C1		2.237	90.35
Canindé (1998ER)	0.904	F2	Temperature	0.286	57.10
		F1		0.850	70.05
		C2		1.298	78.55
		C1		2.137	89.45
Irauçuba (2016ER)	0.855	C1	Temperature	5.588	99.63
		C2		4.444	98.84
		F2		4.154	98.45
Santa Quitéria (2004ER)	0.870	C3	Albedo	232.5	100
		C2	NDVI	-32.08	~0
			Aridity Index	23.8	100
			Temperature	1.822	86.08
		F1	NDVI	-16.67	~0
			Albedo	265.39	100
			Aridity Index	24.68	100
			Temperature	1.511	81.91
		F2	NDVI	-16.36	~0
			Albedo	252.37	100
			Aridity Index	30.03	100
			Temperature	1.027	73.63
Irauçuba Centro Norte (2011ED)	0.788	C1	NDVI	-70.93	~0
			Albedo	196.32	100
			Evapotranspiration	28.53	100
			Precipitation	-30.5	42.43
			Temperature	0.867	70.41
		C2	NDVI	-48.89	~0
			Evapotranspiration	20.41	99.99
			Precipitation	-0.291	42.77
			Temperature	0.709	67.02
		F2	Evapotranspiration	18.33	99.99
			Precipitation	-0.285	42.92
			Temperature	0.993	72.97

~0: value of exponential close to 0

Figure 3 - Desertification Susceptibility Maps in Miraíma (1), Canindé (2), Irauçuba (3), Santa Quitéria (4) and Irauçuba Centro Norte (5)

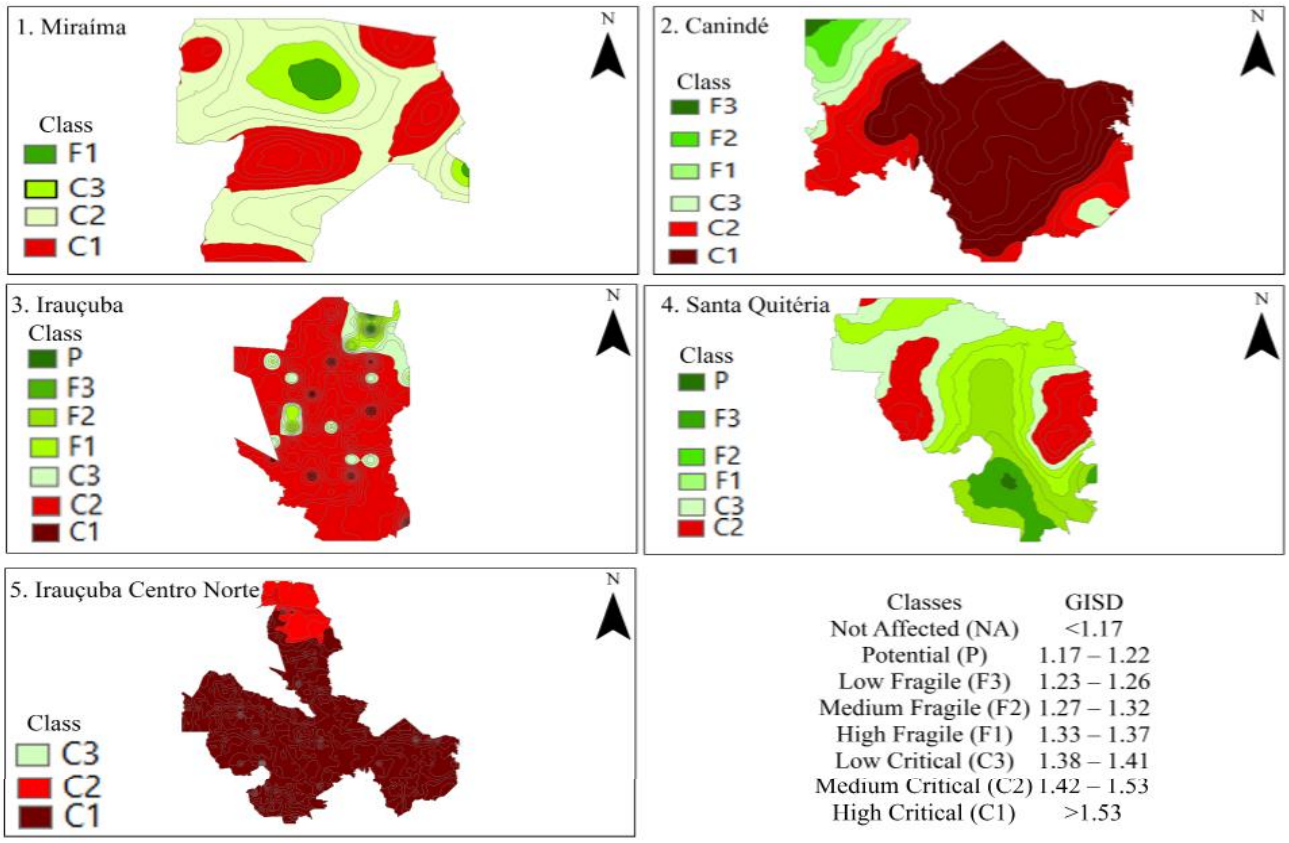

Classes	GISD
Not Affected (NA)	<1.17
Potential (P)	1.17 – 1.22
Low Fragile (F3)	1.23 – 1.26
Medium Fragile (F2)	1.27 – 1.32
High Fragile (F1)	1.33 – 1.37
Low Critical (C3)	1.38 – 1.41
Medium Critical (C2)	1.42 – 1.53
High Critical (C1)	>1.53

For Irauçuba, the GISD for the 2016ER period showed that classes P, F3, F2, F1, C3 and C1 occupied less than 10% of the area of the municipality, while 83.78% was occupied by class C2. According to the MLR model, temperature was significant (p-value < 0.05), with positive coefficients indicating increases in desertification risks of 98.45%, 98.84% and 99.63% in classes F2, C2 and C1, respectively. In class F2, the indices ranged as follows: NDVI (0.4116 – 0.6457); TGSI (0.1983 – 0.3059); albedo (0.0655 – 0.0944); aridity index (0.2596 – 0.2839); precipitation (356.60 mm – 390.04 mm); evapotranspiration (0 – 0.3900 mm/h) and temperature (26.59 °C – 34.54 °C); in relation to class C2, the indices showed the following ranges: NDVI (0.1133 – 0.5353); TGSI (0.0440 – 0.3536); albedo (0.0528 – 0.3113); aridity index (0.2596 – 0.4183); precipitation (356.60 mm – 574.68 mm); evapotranspiration (0 – 0.9113 mm/h) and temperature (7.38 °C – 37.25 °C); in class C1, the indices ranged as follows: NDVI (0.2453 – 0.5156); TGSI (0.1496 – 0.2667); albedo (0.0568 - 0.1331); aridity index (0 – 0.3186); precipitation (0 – 437.62 mm); evapotranspiration (0 – 0.7774 mm/h); and temperature (28.42 °C – 34.53 °C).

In Santa Quitéria, the GISD for the 2004ER period showed that class F1 occupied 28.51% of the territory, followed by C3 with 22.34%, F2 with 20.20% and C2 with 17.79%, while classes P, F3 and C1 occupied less than 10%. The variables NDVI, albedo, aridity index and temperature were significant for classes F2, F1, C3 and C2. NDVI showed a negative coefficient whose exponential tended to values close to zero, indicating a small reduction in the risk of desertification in classes F2, F1 and C2. Albedo and aridity index showed positive coefficients, indicating increases in risks of desertification of 100% for classes F2, F1 and C3 (albedo) and F2, F1 and C2 (aridity index). The increase in temperature resulted in the worsening of the risk of desertification in classes F2, F1 and C2 by 73.63%, 81.91% and 86.08%, respectively.

For class F2, the indices ranged as follows: NDVI (0.3813 – 0.8154); TGSI (0.1257 – 0.6409); albedo (0.0556 – 0.1006); aridity index (0.7473 – 1.2398); precipitation (857.75 mm – 1423 mm); evapotranspiration (0 – 0.9626 mm/h) and temperature (20.28 °C – 37.13 °C); in the F1 class, the indices had the following ranges: NDVI (0.3002 – 0.5145); TGSI (0.1473 – 0.2989); albedo (0.0604 – 0.1170); aridity index (0.7705 – 1.2398); precipitation (884.29 mm – 1423 mm); evapotranspiration (0 – 0.8385 mm/h) and temperature (23.91 °C – 36.31 °C); in C3, the ranges were: NDVI (0.1855 – 0.6429); TGSI (0.1415 – 0.2880); albedo (0.0507 – 0.1372); aridity

index (0.7714 – 1.2398); precipitation (885.37 mm – 1423 mm); evapotranspiration (0 – 0.9531 mm/h) and temperature (23.46 °C – 36.72 °C); in C2, the ranges were: NDVI (0.2083 – 0.2874); TGSI (0.1502 – 0.2054); albedo (0.0900 – 0.1072); aridity index (0.7960 – 0.8100); precipitation (913.56 mm – 929.70 mm); evapotranspiration (0.4508 mm/h – 0.5710 mm/h) and temperature (27.88 °C – 29.61 °C).

The 2011ED period in Irauçuba Centro Norte showed that class C1 occupied more than 90% of the area, followed by C2 with 9.66% and C3 with 0.04%, respectively. NDVI, precipitation, evapotranspiration, temperature and albedo were significant (p-value < = 0.05) for classes F2, C2 and C1. NDVI and Precipitation showed negative coefficients, and NDVI showed a low effect of reduction in the risk of desertification in classes C2 and C1, while precipitation reduced the risk of desertification by 42.92%, 42.77% and 42.43% in classes F2, C2 and C1, respectively. Albedo increased the risk of desertification by 100% for C1 and evapotranspiration increased it by 99.99% to 100% for F2, C2 and C1, while temperature increased the risk of desertification by 72.97%, 67.02% and 70.41%, respectively.

The descriptive analysis of the indices showed that in F2 they ranged as follows: NDVI (0.4567 – 0.6642); TGSI (0.1572 – 0.2373); albedo (0.0849 – 0.0982); evapotranspiration (0.1643 – 0.4061); temperature (31.22 °C – 34.21 °C); aridity index (0.1550 – 0.1713) and precipitation (158.07 mm – 174.72 mm); in C2, the ranges were: NDVI (0.4023 – 0.7723); TGSI (0.1426 – 0.3660); albedo (0.0281 – 0.1339); evapotranspiration (0 – 0.6627 mm/h); temperature (26.74 °C – 38.71 °C); aridity index (0 – 0.1770) and precipitation (0 – 180.53 mm); for C1, the indices ranged as follows: NDVI (0.1104 – 0.6018); TGSI (0.0470 – 0.5055); albedo (0.0097 – 0.2429); evapotranspiration (0 – 0.9002 mm/h); temperature (25.60 °C – 40.52 °C); aridity index (0 – 0.1772) and precipitation (0 – 180.72 mm).

NDVI and Precipitation were significant in reducing the risk of desertification in Santa Quitéria and Irauçuba Centro Norte, and NDVI showed little effect in reducing the risk of desertification in F2, F1, C2 and C1 for both areas. Precipitation reduced the risk of desertification by 42.9%, 42.7% and 42.4% in F2, C2 and C1, respectively, in Irauçuba Centro Norte. Albedo, temperature, aridity index and evapotranspiration increased the risk of desertification by 67.02% to 100% for Santa Quitéria and Irauçuba Centro Norte.

The association of NDVI and Precipitation in reducing the risk of desertification in semi-arid areas is due to the contribution of moisture to the soil, which can improve vegetation cover and minimize the effects of drought by reducing temperature and increasing precipitation, reducing the risk of desertification (Dameneh *et al.*, 2021). In Santa Quitéria and Irauçuba Centro Norte, the correlations were -0.9578 and -0.6035 between NDVI and Albedo, respectively, -0.5233 and -0.6371 between NDVI and temperature, respectively, -0.8252 and -0.7555 between NDVI and GISD, respectively. The reduction of albedo results in greater absorption of solar radiation by plants and lower soil reflectance, favoring lower temperatures and higher precipitation. In Santa Quitéria and Irauçuba Centro Norte, the correlations were 0.6515 and 0.5517 between albedo and temperature, respectively, -0.8028 and -0.5169 between albedo and precipitation, respectively, and 0.7358 and 0.4986 between albedo and GISD, respectively.

Temperature was significant in Miraíma, Canindé, Irauçuba and Santa Quitéria (local scale) and in Irauçuba Centro Norte (global scale); it was observed that the increase in temperature caused the risks of desertification to vary between 54.25% and 98.45% in the fragile class and between 67.02% and 99.63% in the critical class. Critical areas were the most affected by the increase in temperature, as a result of the higher stage of degradation of these areas, which recorded increments of more than 90% in areas occupied by pastures, fires, and pastures degraded by overgrazing (Souza *et al*., 2020).

Irauçuba and Santa Quitéria were the municipalities most affected by the temperature changes; the increase of 1 degree Celsius aggravated the risks of desertification by 98.45% to 99.63% in Irauçuba and 81.91% to 86.08% in Santa Quitéria. For these areas, the use and occupation of the land without considering conservational aspects aggravated desertification, as there were increase in stocking rates by 69% between 2000 and 2006 in Irauçuba and deforestation peaks in 2004 and 2007 for Santa Quitéria, which has the highest deforestation rates in Ceará (Ferreira *et al*., 2018; Santos *et al*., 2021).

The permanent use and occupation of the land based on anthropic practices with low technological level and conservation of fauna and flora considerably reduced the spectral responses of the vegetation and increased the spectral response of the soil, since the removal of vegetation with fire for the occupation of pastures subjected to overgrazing in soils of restricted use resulted in compaction and degradation, leading to less support for vegetation cover and organic matter input, lower moisture retention and thermal stability of the soil, affecting the conditions of energy balance between the soil and atmosphere due to changes in albedo and temperature (Ferreira *et al*., 2018; Santos *et al*., 2021).

Fires have been correlated with the advance of desertification in Caatinga areas, since the increase in soil

surface temperature results in the destruction of organic matter, volatilization of organic compounds, reduction of soil carbon and infiltration rates, and increase of water erosion, leading to soil impoverishment and lower capacity for vegetation regeneration, followed by the worsening of desertification (Lucas-Borja *et al*., 2022; Pivello *et al*., 2021).

The assessment of desertification risk on global, local and hierarchical scales showed that the degradation of vegetation and soil quality altered the climatic conditions due to changes in the energy balance between soil and atmosphere and in the rainfall regime, increasing the risk of desertification. The averages of NDVI and precipitation decreased between 56.3% and 87.7%, while those of albedo and temperature increased between 29.3% and 47.3%. The present study showed that the correlations ranged from -0.6035 to -0.9358 between NDVI and albedo, from -0.2263 to -0.7644 between NDVI and temperature, from 0.4324 to 0.7442 between temperature and albedo, and -0.1546 to -0.9711 between temperature and precipitation.

The increase in albedo and temperature can favor the increase of sensible heat flux, reducing precipitation; on the other hand, the reduction of albedo and temperature contribute to an increase in latent heat flux, increasing the probability of precipitation and reducing the risks of desertification (Djeddaoui; Chadli; Gloaguen, 2017; Ning *et al*., 2021; Zolotokrylin; Brito-Castillo; Titkova, 2020).

CONCLUSIONS

1. The multinomial logistic regression models showed better performances in the assessment of desertification risk for the end of the rainy season and at the local scale;
2. NDVI and precipitation may contribute to reducing the risk of desertification in Santa Quitéria and Irauçuba Centro Norte, while albedo, temperature and evapotranspiration aggravate the risk;
3. The increased risk of desertification on global, local and hierarchical scales is associated with changes in temperatures that have affected the microclimate and reduced precipitation.

ACKNOWLEDGMENTS

The authors would like to thank the Coordination for the Improvement of Higher Education Personnel (CAPES) and the Group for Automation in Agricultural Management – Technological Development (GAMA - DT) for the intellectual and financial support and the Pro-Integration project for the resources.

REFERENCES

DAMENEH, H. E. *et al.* Desertification of Iran in the early twenty-first century: assessment using climate and vegetation indices. **Scientific Reports**, v. 11, p. 1-18, 2021.

DJEDDAOUI, F.; CHADLI, M.; GLOAGUEN, R. Desertification susceptibility mapping using logistic regression analysis in the Djelfa area, Algeria. **Remote Sensing**, v. 9, p. 1-26, 2017.

FERREIRA, M. P. S. *et al.* Changes in attributes of soils subjected to fallow in desertification hotspot. **Revista Ciência Agronômica**, v. 49, p. 1-31, 2018.

FUNDAÇÃO CEARENCE DE METEOROLOGIA E RECURSOS HÍDRICOS. **Zoneamento ecológico-econômico das áreas susceptíveis à desertificação do núcleo I Irauçuba/ Centro-Norte**. Fortaleza, 2015.

KARAMESOUTI, M.; PANAGOS, P.; KOSMAS, C. Model-based spatio-temporal analysis of land desertification risk in Greece. **Catena**, v. 167, p. 266-275, 2018.

KOSMAS, C.; KIRKBY, M.; GEESON, N. **Manual on key indicators of desertification and mapping environmentally sensitive areas to desertification.** European Commission, Energy, Environment and Sustainable Development, 1999.

LI, P. *et al*. Dynamic monitoring of desertification in Ningdong based on Landsat images and machine learning. **Sustainability**, v. 14, p. 1-35, 2022.

LI, G. *et al.* Modeling potential impacts on regional climate due to land surface changes across Mongolia plateau. **Remote Sensing**, v. 14, p. 1-15, 2022.

LUCAS-BORJA, M. E. *et al.* Exploring the factors influencing the hydrological response of soil after low and high-severity fires with post-fire mulching in Mediterranean forests. **International Soil And Water Conservation Research**, v. 10, p. 1-14, 2022.

MIHI, A.; GHAZELA, R.; WISSAL, D. Mapping potential desertification-prone areas in North-Eastern Algeria using logistic regression model, GIS, and remote sensing techniques. **Environmental Earth Sciences**, v. 81, p. 1-14, 2022.

NING, Z. *et al*. Plant community C: n. **Ecological Engineering**, v. 162, p. 1-12, 2021.

PEREZ-MARIN, A. M. *et al*. Monitoring desertification using a small Set of biophysical indicators in the brazilian semiarid region. **Sustainability**, v. 14, p. 1-24, 2022.

PIVELLO, V. R. *et al.* Understanding Brazil's catastrophic fires: causes, consequences and policy needed to prevent future tragedies. **Perspectives In Ecology And Conservation**, v. 19, p. 1-23, 2021.

SANTOS, T. C. S. *et al*. Detecting desertification in different years and rainfall regimes by 2D Scatter Plot. **Revista Ciência Agronômica**, v. 52, p. 1-10, 2021.

SHARMA, L. K.; RAJ, A.; SOMAWAT, K. Spatio-temporal assessment of Environmentally Sensitive Areas (ESA) in The

Thar Desert India, to combat desertification under UNCCD framework. **Journal of Arid Environments**, v. 194, p. 1-17, 2021.

SOUSA, F. P. *et al*. Carbon and nitrogen in degraded Brazilian semi-arid soils undergoing desertification. **Agriculture, Ecosystems & Environment, v.** 148, p. 11-21, 2012.

SOUZA, C. M. *et al*. Reconstructing three decades of land use and land cover changes in Brazilian biomes with Landsat archive and Earth Engine. **Remote Sensing**, v. 12, p. 1-27, 2020.

UZUNER, C.; DENGIZ, O. Desertification risk assessment in Turkey based on environmentally sensitive areas. **Ecological Indicators**, v. 114, p. 1-12, 2020.

XU, D.; YOU, X.; XIA, C. Assessing the spatial-temporal pattern and evolution of areas sensitive to land desertification in North China. **Ecological Indicators**, v. 97, p. 150-158, 2019.

ZOLOTOKRYLIN, A. N.; BRITO-CASTILLO, L.; TITKOVA, T. B. Local climatically-driven changes of albedo and surface temperatures in the Sonoran Desert. **Journal of Arid Environments**, v. 178, p. 1-13, 2020.